Systems & Control Transactions

Original Research Article
Peer Reviewed Conference Proceeding
ESCAPE 36 - European Symposium on Computer Aided Process Engineering
Sheffield, UK. 21-24 June 2026

PSE PRESS

Real-Time Estimation and Optimal Control of Supersaturation in Sugar Crystallization using Model-based Soft Sensor

Ananya Lohani[a]*, Adam Fedor[a], Július Kurucz[b], and Radoslav Paulen[a]

[a] Faculty of Chemical and Food Technology, Slovak University of Technology in Bratislava, 812 37 Bratislava, Slovakia
[b] FUZZY s.r.o., 925 81 Diakovce, Slovakia
* Corresponding Author: ananya.lohani@stuba.sk.

ABSTRACT

Maintaining mother liquor supersaturation at a setpoint within the metastable range is vital for achieving the best production yield in industrial sugar production. However, precise online measurement and control is challenging. In this work, we develop a model-based soft sensor for supersaturation monitoring, and we propose a new feedforward-feedback control structure for batch sugar crystallization. Supersaturation is estimated using standard process measurements, enabling a soft sensor that can be readily adapted to different production units. The soft sensor continuously estimates supersaturation from standard process signals, and the control strategy ensures it remains within the desired operating range, enabling simple and straightforward application to other sugar production units.

Keywords: Mass Balance, Energy Balance, Soft Sensor, Feedback Control, Feedforward Control, Supersaturation

INTRODUCTION

Sugar crystallization is a crucial unit operation in the sugar manufacturing industry, directly influencing the yield and quality of product, and overall process efficiency [1]. Supersaturation is one of the key variables determining crystallization performance, as it regulates crystal growth, nucleation behaviour, and dissolution phenomena. It must be maintained within the metastable zone, typically in the range of $1.00 < \sigma < 1.35$ for the best yield and quality of sugar [2]. Operating outside this window may result in the excessive nucleation, crystal agglomeration, or dissolution, leading to reduced sugar recovery and off-spec crystal size distribution.

Despite its significance, supersaturation is challenging to measure online in industrial crystallizers due to its reliance on several major factors, like temperature, concentration (Brix), purity of the mother liquor, and pressure [3]. As direct measurement is not viable, industrial practice largely relies on indirect indicators, operator experience, or exclusive instruments. At present, the SeedMaster series transmitter [4] is the only commercially available instrument that provides an online estimation of supersaturation. Its applicability is, however, limited by cost, proprietary algorithms, and lack of integration with advanced feedback control strategies.

Several research efforts have addressed the estimation and regulation of other hard-to-measure process properties, such as crystal size distribution and solution conductivity, which are closely linked to supersaturation and can be viewed as different expressions of the same crystallization behaviour, to improve the sugar yield quality using data-driven, model-based, and hybrid soft sensors. Data-driven approaches offer major advantages while capturing complex, non-linear process behaviour using historical or online plant data, thereby improving prediction accuracy without requiring detailed physical descriptions. Leveraging these benefits, Devogelaere et al. [5] demonstrated the use of feedforward neural networks as soft sensors for predicting massecuite electrical conductivity that serves as an indicator of supersaturation, supporting real-time control setpoint adjustments. Likewise, Lu et al. [6] presented an online modeling technique based on multi-input multi-output partial least-

squares support vector machines, achieving simultaneous estimation of massecuite brix and supersaturation.

Model-based approaches contribute to improved interpretability by incorporating fundamental physical relationships into the process description. Bakir et al. [7] proposed a continuous-discrete observer for estimating crystal size distribution in batch crystallization using a reduced population balance equation model. This formulation enables real-time monitoring while supporting control of filterability and flowability. Similarly, Damour et al. [2] introduced a model-based soft sensor for C-stage crystallization, providing online estimates of crystal mass, sucrose concentration, and purity aimed at maximizing sugar exhaustion.

Despite the advantages of data-driven and model-based approaches, their performance is often limited in crystallization processes involving high impurity levels and complex kinetic behaviour. Model-based approaches often suffer from parameter uncertainty, whereas data-driven models typically lack robustness, physical interpretability, and extrapolation capability beyond their training domain. Hybrid modeling frameworks address these limitations by merging mechanistic equations with data-driven components, enabling accurate representation of complex phenomena with limited data requirements. Georgieva et al. [8] proposed a knowledge-based hybrid model for fed-batch crystallization, integrating mass, energy, and population balance equations with artificial neural networks to accurately describe growth, nucleation, and agglomeration processes. Similarly, Meng et al. [9] demonstrated the applicability of data-driven and hybrid models for online estimation of supersaturation, mother liquor purity, crystal content, and crystal size distribution.

Despite the significant progress in data-driven, model-based, and hybrid soft-sensing techniques, their utilization in closed-loop control structures remains limited in industrial environments. The complexity of crystallization kinetics, coupled with uncertainty in process parameters and industrial implementation constraints, has limited the transition from monitoring to active control. Consequently, industrial sugar crystallization processes continue to rely mainly on conventional PI controllers for regulation of level and temperature, while the true control objective—maintaining supersaturation within the metastable zone- is only indirectly addressed through these variables. To the best of the authors' knowledge, no recorded studies have implemented a feedback control framework that explicitly manages supersaturation within the metastable range using model-based estimation. This represents a significant gap, particularly given the increasing demand for improved energy efficiency, higher extraction rates, and consistent product quality in sugar factories [10].

In this work, a model-based soft sensor is utilized to explicitly estimate supersaturation using mass and energy balance equations, incorporating key process variables such as purity, crystal mass, temperature, and concentration. Furthermore, supersaturation is directly regulated through a combined feedback-feedforward control strategy based on a standard PID controller, with the feed flow rate and heating steam supply rate considered as the manipulated inputs. The strength of this study lies in the practical use of simple, well-established control techniques to explicitly estimate and control supersaturation, thereby bridging the gap between theoretical approaches and industrial implementation. Overall, the proposed framework enables online supersaturation estimation and regulation without reliance on specialized measurement systems, offering a practical and industry-ready solution.

THEORY

This section is focused on the development of a model-based soft sensor of supersaturation using mass and energy balance equations.

Mass and Energy Balance Equations

The C-stage crystallization process is modelled using the set of five ordinary differential equations, with only the operating conditions and parameter values adjusted to reflect the C-stage operation [2], [12].

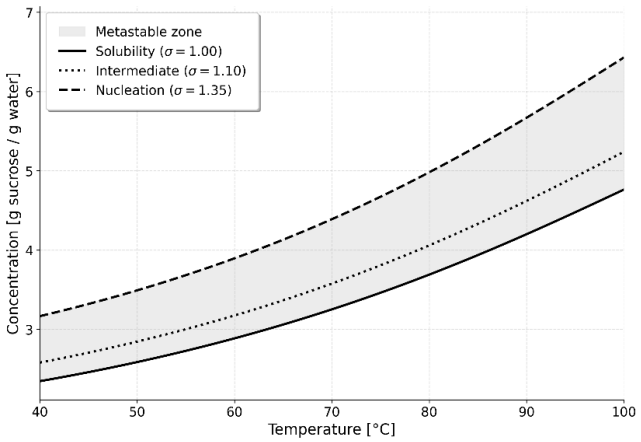

Figure 1. Temperature-dependent solubility curve of sucrose [13]

$$\frac{dm_w}{dt} = \rho_{feed} F_{feed}(1 - Bx_{feed}) - \dot{m}_{vap} \quad (1)$$

$$\frac{dm_i}{dt} = \rho_{feed} F_{feed} Bx_{feed}(1 - Pur_{feed}) \quad (2)$$

$$\frac{dm_c}{dt} = cc\left(\rho_{feed} F_{feed} - \dot{m}_{vap}\right) + \alpha_c \quad (3)$$

$$\frac{dm_s}{dt} = (\rho_{feed} F_{feed} Bx_{feed} Pur_{feed}) - \frac{dm_c}{dt} \quad (4)$$

$$\frac{dT_{mag}}{dt} = \frac{W + Q_{hs} + \rho_{feed} F_{feed}(h_{feed} - h_{ml}) - \dot{m}_{vap} L_{vap} + \frac{dm_c}{dt} L_c}{m_{total} Cp_{mag}} \quad (5)$$

Table 1. summarizes the typical operating conditions of an industrial sugar crystallization. Throughout the work, the subscript 'feed' refers to properties associated with the inlet feed stream. Here m_w, m_i, m_c and m_s denote the masses of water, impurities, crystal and dissolved sucrose, respectively. The feed density is depicted by ρ_{feed}, while F_{feed} represents the feed flow rate. The stirring power W is fixed at 15 kW. In addition, h denotes the specific enthalpy, L the specific latent heat, and Cp_{mag} the specific heat capacity of magma. $\dot{m}_{vap}$ represents mass flow rate of emitted vapour which is defined as $\dot{m}_{vap} = \rho_{cw} F_{vap}$, where ρ_{cw} is the density of condensed water and F_{vap} the emitted vapour mass flow rate, m_{total} the total mass in the magma and is defined as $m_{total} = m_c + m_w + m_i + m_s$, and Q_{hs} the heating power which is brought by the condensation of heating steam and defined as $Q_{hs} = \rho_{cw} F_{cs} L_{cw}$. All the thermal and physical correlations are mentioned below in the appendix. The RHS of eq (3) is the crystallization rate, which is calculated using the moment equations computed from the population balance equations, where cc is the crystal content which can be defined as $cc = m_c/m_{total}$ and α_c is an adjusted parameter according to crystal growth kinetic [14]. All the typical operating conditions are mentioned in Table 1.

Table 1: Typical operation conditions of a sugar plant [12]

Parameter	Description	Values
p_v	Vacuum Pressure	$0.12 - 0.15$ bar
Bx_{feed}	Feed Brix	$72 - 76°$ Bx
Bx_{mag}	Magma Brix	$88 - 95°$ Bx
Pur_{feed}	Feed Purity	$70 - 75\%$
Pur_{mag}	Magma Purity	$60 - 65\%$
Pur_{ml}	Mother Liquor Purity	$0 - 65\%$
T_{mag}	Magma Temperature	$60 - 75$°C
T_w	Water Temperature	$60 - 65$°C
T_{feed}	Feed Temperature	$60 - 65$°C

Direct measurement of gas flow rates in industrial equipment is typically infeasible. Consequently, both the heating steam and emitted vapour flow rates are commonly computed through indirect measurements using simplifying assumptions. The authors [2] suggest simplifying involved heat and mass transfer phenomena by introducing simplifications in a form of correlation factors α

1. First, the dynamics between heating steam supply flow rate F_{hs} and condensed steam F_{cs} is considered negligible with respect to the kinetics of the process. Thus:

$$F_{hs} = \alpha_Q F_{cs} \tag{6}$$

2. Second, the emitted vapor flow rates F_{vap} is proportional to the condensed steam flow rate F_{cs} via:

$$F_{vap} = \alpha_{vap} F_{cs} \tag{7}$$

The model framework is strictly governed by mass and energy conservation laws, utilizing standardized correlations (in Appendix) for the enthalpy and density of technical sugar solutions.

Supersaturation in crystallization processes

Supersaturation is described as the ratio between the mass of sucrose to the mass of water contained in a supersaturated solution ($s = m_s/m_w$) and the mass of the sucrose to the mass of the water which would be present in a saturated solution (s_{sat}) at the same temperature and purity [9], [15].

$$SS = \frac{s}{s_{sat} C_{sol}} \tag{8}$$

For a pure saturated solution, it is known that s_{sat} depends on temperature via the brix at saturation Bx_{sat}: [13]

$$s_{sat} = \frac{Bx_{sat}}{100 - Bx_{sat}} \tag{9}$$

However, considering the presence of impurities in industrial sucrose solutions, the s_{sat} is adjusted through the introduction of a solubility coefficient C_{sol}. The solubility coefficient is a parameter representing the impact of impurities on sucrose solubility. Several researchers have proposed correlations to calculate it [10], [12]. In this work, C_{sol} is determined by the well-known empirical correlation,

$$C_{sol} = a \frac{m_i}{m_w} + b + (1 - b) e^{-c \frac{m_i}{m_w}} \tag{10}$$

where a, b and c are quality parameters of the mother liquor that depend on the amount and composition of local impurities.

Since supersaturation cannot be measured directly and is driven by the strongly interacting dynamics of concentration and temperature [11], the adopted formulation offers a practical and transparent estimation strategy suitable for industrial crystallization processes.

METHODOLOGY

The proposed model is validated through numerical simulations using synthetic datasets embedded with Gaussian noise to mimic industrial conditions. The flow rate of feed F_{feed} and heating steam supply F_{hs} are implemented as time-varying, piecewise-constant inputs. This strategy ensures controlled supersaturation while maintaining temperature and level % for model validation.

Given the complexity of the multivariable system, we determined the kinetic parameters using well-established thermodynamic definitions and empirical

correlations reported in the literature (Appendix)[2], [10]. To evaluate the sensitivity of the estimated α parameters to experimental noise, a Monte Carlo Simulation was performed [16]. For each iteration, the parameter set was re-estimated using a Levenberg-Marquardt least-squares minimization (8). This process allows the uncertainty and correlation between parameters to be analyzed.

Here for $\mathrm{Bx}_{ml,exp}$, $\mathrm{Bx}_{mag,exp}$, and $T_{mag,exp}$, we used simulated measurements with added gaussian noise to mimic experimental variability. The parameters are determined by minimizing the difference between these noisy "experimental" values and the corresponding model predictions.

$$\min_{\alpha_c,\alpha_{vap},\alpha_Q} \left(\frac{1}{2}\sum_{j=1}^{N}\left(Bx^{j}_{ml,exp} - \mathrm{Bx}^{j}_{ml,sim}\right)^2 + \frac{1}{2}\sum_{j=1}^{N}\left(\mathrm{Bx}^{j}_{mag,exp} - \mathrm{Bx}^{j}_{mag,sim}\right)^2 + \frac{1}{2}\sum_{j=1}^{N}\left(T^{j}_{mag,exp} - T^{j}_{mag,sim}\right)^2\right) \quad (11)$$

To determine the optimal vector of coefficients, present in supersaturation equation $\theta = [a, b, c]$, a minimization problem is solved using Nelder-Mead optimization algorithm, based on values reported in previous literature. The goal is to align the model's calculated supersaturation at the final batch state with a target supersaturation value ($S_{target} = 1.10$). The targeted supersaturation value is taken from industrial perspective. The objective function, $J(\theta)$, is defined as the sum of the squared error between the calculated and target supersaturation, plus a regularization term, which is added so to keep the estimated value closer to the values available in previous literature [12]:

$$J(\theta) = \left(S_{calc}(\theta) - S_{target}\right)^2 + \lambda \sum_{i\in a,b,c}\left(\theta_i - \theta_{prior}\right)^2 \quad (12)$$

Where $S_{calc}(\theta)$ is the supersaturation computed using the trial parameters, λ is a penalty weight and θ_{prior} represents the original estimates for the coefficients which are taken from the previous literature [10].

Note that these parameters vary from plant to plant, depending on plant design and operating conditions.

Table 3: Model parameters and their values

Parameter	Values
α_{vap}	0.98
α_Q	1.65
α_c	0.29
a	-0.00573
b	1.00939
c	2.09860

Control strategy

Soft sensor will act as a feedforward part of the controller adjusting the supersaturation measurement with respect to the disturbances such as impurities, variations in temperature, etc. For feedback control procedure, a PID controller is implemented to regulate the supersaturation level inside the batch crystallizer. The control objective is to track a target supersaturation setpoint while compensating for disturbances induced by evaporation and non-linear solubility dynamics.

Here SS is the controlled variable, whereas F_{feed} is the manipulated variable. The supersaturation tracking error is defined as:

$$e(t) = SS_{target} - SS(t) \quad (13)$$

Where SS_{target} is the desired supersaturation setpoint.

The feed flow rate $F_{\mathrm{feed}}(t)$ is calculated using a standard PID algorithm. The control effort relies entirely on the error dynamics and the integral accumulation to sustain the flow.

$$F_{\mathrm{feed}}(t) = K_p e(t) + K_i \int_0^t e(\tau)\,d\tau + K_d \frac{de(t)}{dt} \quad (14)$$

Where K_p, K_i, and K_d are the proportional, integral, and derivative gains, respectively, and are tuned based on simulation studies [17], [18].

In practice, the controller is implemented in discrete time, with the integral and derivative terms in equation (15) approximated numerically at each sampling instant. The heating steam supply rate $F_{hs,forw}$ is applied as a feedforward control signal, based on typical operating settings. To ensure the physical realism, the actual flow rate of feed $F_{\mathrm{feed}}(t)$ applied to the crystallizer is subject to three specific constraints implemented in the simulation:

1. Integral Anti-Windup: To prevent excessive accumulation of error during saturation, the integral term is clamped to a fixed range chosen based on simulation studies and K_i value [19]:

$$-20 \le \int_0^t e(\tau)\,d\tau \le 20 \quad (15)$$

2. Actuator Rate Limiting: The model limits how quickly the feed valve can open or close. The change in output (Δu) per time step is constrained by a maximum rate ($R_{max} = 0.0001$) for smooth control of the manipulated input. [20]

$$|F_{\mathrm{feed}}(t) - F_{\mathrm{feed}}(t - \Delta t)| \le R_{max} \quad (16)$$

3. Output Saturation: The final flow rate is bounded by the physical limitations of the valve (minimum and maximum flow):

$$F_{\mathrm{feed},min} \le F_{\mathrm{feed}}(t) \le F_{\mathrm{feed},max} \quad (17)$$

4. Shutdown logic: To be in safety thermal limit and level%, the system calculates a dimensionless Shutdown factor, denoted as $\alpha(L)$, which is the function of the crystallizer level percentage $L(t)$. This factor is used to ramp down the steam injection and trigger a

hard stop for the feed.

$$\alpha(L) = \begin{cases} 1.0 & if\ L(t) < 98.0\% \\ \frac{99.5 - L(t)}{99.5 - 98.0} & if\ 98.0\% \le L(t) < 99.5\% \\ 0.0 & if\ L(t) \ge 99.5\% \end{cases} \quad (18)$$

The steam flow rate, which normally follows a step-change Feed forward control $F_{hs,forw}$, is directly multiplied by this factor. This gradually reduces evaporation energy as the tank fills, preventing overheating at the end of the batch:

$$F_{hs}(t) = F_{hs,forw}(t) \times \alpha(L) \quad (19)$$

The feed flow is controlled by the PID loop described above, but it is subject to a separate "Hard Safety Cutoff" strictly when the tank reaches maximum capacity:

$$F_{feed}(t) = \begin{cases} 0.0 & if L(t) \ge 100 \\ u_{PID}(t) & otherwise \end{cases} \quad (20)$$

Without such constraints, the controller becomes aggressive, producing control actions that violate physical realism. This can lead to excessive dilution or overheating, ultimately degrading crystak quality. Variations in F_{feed} affect the water content and dissolved sucrose concentration, which in turn alter the supersaturation level.

The control strategy was implemented during the batch crystallization, and its performance was evaluated by tracking the evolution of supersaturation, magma temperature, and mass components.

RESULTS

The simulation was conducted over a batch duration of 8 hours (28800 seconds) with a sampling integration step (Δt) of 10 seconds.

For α parameter sensitivity and robustness, a Monte Carlo simulation with 200 iterations was performed, introducing 2% gaussian noise to the nominal simulation data. The results (Figure 2) present the pairwise correlation plots, which illustrate the robustness of the estimated α parameters. Most of the 200 parameters estimates are tightly clustered around the true value, indicated by the red marker, showing that not only the Levenberg-Marquardt algorithm reliably avoids convergence to local minima but also that the parameters are well-identifiable.

A correlation analysis was conducted to examine the relationship among α_Q, α_{vap}, and α_c. The results indicate a moderate negative correlation between α_Q and α_{vap} $(r = -0.65)$, and a strong negative correlation between α_Q and α_c $(r = -0.93)$. In contrast, α_{vap} and α_c exhibit a strong positive correlation $(r = 0.88)$. The correlation results can be justified by looking at Eq. (3). The parameters mutually align to accurately track crystal mass accumulation. Table 2. suggests that the estimation procedure is numerically stable and that the identified parameters are robust with respect to uncertainty and noise in the data.

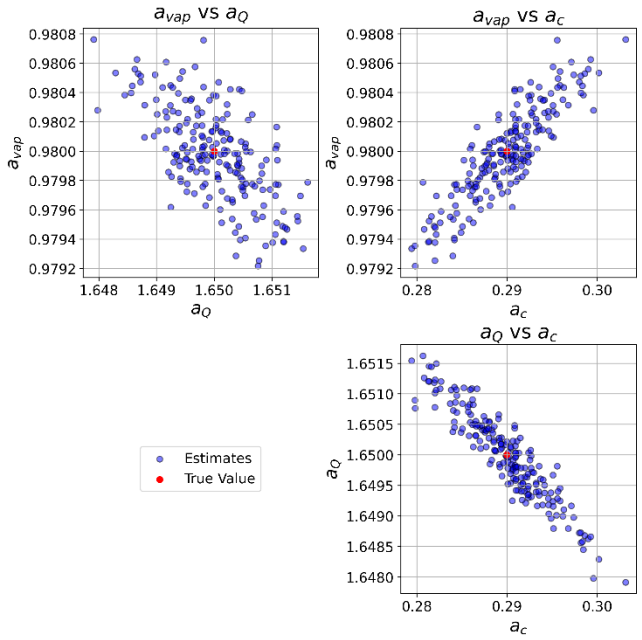

Figure 2. Pairwise parameter correlations ($N = 200$ and noise= 2%)

Table 2. Parameter estimation statistics

Parameter	Mean	Standard deviation
α_c	0.2899	0.0045
α_{vap}	0.9800	0.0003
α_Q	1.6500	0.0007

The impurity-dependent coefficients a, b, and c in the supersaturation were estimated via Nelder-Mead optimization algorithm (12). Estimated values are mentioned in Table 3. The resulting coefficients were subsequently validated by confirming that the simulated supersaturation dynamics and temperature-dependent solubility profiles aligned with consistent physical behaviour.

The controller performance was analyzed in terms of its ability to regulate supersaturation close to the desired operating region despite varying thermal conditions and changing liquor composition. Since the feedforward heating steam supply flow rate is not violating safety limits, hence the $\alpha(L) = 1$, which concludes that $F_{hs} = F_{hs,forw}$ here (Figure 3.)

The results (figure 3.) indicate that the control strategy provides smooth and stable trajectories, avoiding abrupt oscillations in supersaturation and temperature that could otherwise compromise crystal growth with the supersaturation profile remaining predominantly within the metastable region, indicating that the interaction

between feed addition and evaporation is well balanced. Brief disturbances are observed primarily during adjustment of steam flows; however, these deviations are short-lived and do not lead to uncontrolled nucleation or crystal dissolution. The results are further validated in the solubility curve Figure 3.

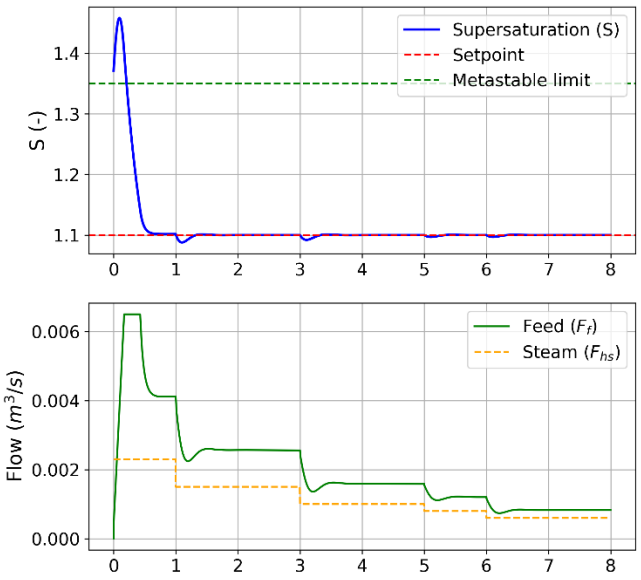

Figure 3. Control performance: supersaturation over time (top), manipulated variables (bottom). In addition, the controlled feed policy results in a gradual and consistent increase in crystal mass, reflecting favorable growth-dominated conditions. The absence of sharp oscillations in supersaturation and temperature suggests that the controller effectively mitigates process non-linearities and time-varying behavior inherent to batch crystallization.

Overall, the dynamic profiles indicate a stable operating regime that supports uniform crystal growth and improved product quality. The magma temperature varies within safe thermal limits across a wide operating range, indicating that the proposed soft sensor and control strategy operate effectively under different thermal conditions and maintain proper regulation of the energy balance through coordinated feed-flow control.

CONCLUSION AND FUTURE WORK

This study shows that supersaturation in batch sugar crystallization can be effectively regulated using constrained feedback control of the feed flow rate combined with feedforward steam supply. The proposed dynamic model captures the coupled mass and energy balances and maintains supersaturation within the metastable range under stable operation. Thermodynamic inconsistencies in commonly used parameter correlations were resolved, resulting in a physically consistent and numerically robust framework. Simulation results reproduce key industrial trends, indicating strong potential for practical application. Future work will focus on parameter estimation using real plant data to further improve predictive accuracy and assess robustness under realistic operating conditions.

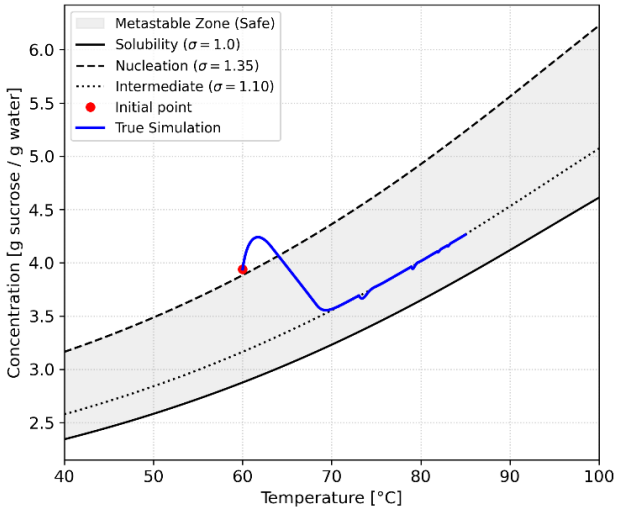

Figure 4. Feedback control effect on the solubility curve

APPENDIX

Brix and Purity for mother liquor and magma

$$\mathrm{Bx}_{ml} = \frac{m_i + m_s}{m_w + m_i + m_s}$$

$$\mathrm{Bx}_{mag} = \frac{m_i + m_{c_{m_s}}}{m_w + m_i + m_c + m_s}$$

$$\mathrm{Pur}_{ml} = \frac{m_s}{m_i + m_s}$$

$$\mathrm{Pur}_{mag} = \frac{m_c + m_s}{m_i + m_c + m_s}$$

Density (in $\mathbf{kg/m^3}$)

$$\rho_{\mathrm{feed}} = \left(1000 + \frac{(100Bx_{\mathrm{feed}})(200 + (100Bx_{\mathrm{feed}}))}{54}\right)\left(1 - 0.036\frac{T_{\mathrm{feed}} - 20}{160 - T_{\mathrm{feed}}}\right) - \left(1 - e^{(1-Pur_{\mathrm{feed}})(1.164\times10^{-4}(100Bx_{\mathrm{feed}}) + 6.927\times10^{-6}(100Bx_{\mathrm{feed}})^2)}\right)$$

$$\rho_{cw} = 1016.7 - 0.57T_w$$

Specific heat capacity (in $\boldsymbol{J/(kgK)}$)

$$Cp_{mag} = 4187 - 29.309Bx_{mag}$$

$$Cp_c = 1163.2 - 3.488T_{mag}$$

$$Cp_{ml} = 4186.8 - 29.7Bx_{ml} + 4.61Bx_{ml}Pur_{ml} + 0.075Bx_{ml}T_{mag}$$

$$Cp_{\text{feed}} = 4186.8 - 29.7Bx_{\text{feed}} + 4.61Bx_{\text{feed}}Pur_{\text{feed}} + 0.075Bx_{\text{feed}}T_{\text{feed}}$$

Specific enthalpy (in J/kg)

$$h_{\text{feed}} = Cp_{\text{feed}}T_{\text{feed}}$$

$$h_{ml} = Cp_{ml}T_{mag}$$

$$h_c = Cp_cT_{mag}$$

$$h_w = 2323.3 + 4106.7T_w$$

$$h_{vap} = 2499980 - 24186p_v + (1891.1 + 106.1p_v)T_v$$

Specific latent heat (in J/kg)

$$L_c = h_{ml} - h_c$$

$$L_{vap} = h_{vap} - h_w$$

Brix at Saturation

$$Bx_{sat} = 64.447 + 0.08222T_{mag} + 1.6169 \times 10^{-3}T_{mag}^2 - 1.558 \times 10^{-6}T_{mag}^3 - 4.63 \times 10^{-8}T_{mag}^4$$

ACKNOWLEDGEMENT

This work is funded by the Slovak Research and Development Agency under the project APVV-24-0007 and by the Scientific Grant Agency of the Slovak Republic under the grant 1/0263/25, and by the European Union under the grant scheme NextGenerationEU project no. 09I01-03-V05-00002.

REFERENCES

1. RICHARDSON JF, HARKER JH, BACKHURST JR. Crystallisation. Chemical Engineering :827-900 (2002). https://doi.org/10.1016/b978-0-08-049064-9.50026-6
2. Damour C, Benne M, Grondin-Perez B, Chabriat JP. Soft-sensor for industrial sugar crystallization: on-line mass of crystals, concentration and purity measurement. Control Engineering Practice 18:839-844 (2010). https://doi.org/10.1016/j.conengprac.2010.03.005
3. Damour C, Benne M, Boillereaux L, Grondin-Perez B, Chabriat JP. Multivariable linearizing control of an industrial sugar crystallization process. Journal of Process Control 21:46-54 (2011). https://doi.org/10.1016/j.jprocont.2010.10.002
4. L. Rózsa, J. Rózsa, Z. Ltd, S. Kilpinen, E. Mielonen, and K.-P. Oy, “Selection of the Operating Parameters in Sugar Crystallization Control”.
5. Devogelaere D, Rijckaert M, Leon OG, Lemus GC. Application of feedforward neural networks for soft sensors in the sugar industry. VII Brazilian Symposium on Neural Networks, 2002. SBRN 2002. Proceedings. :2-6 (None). https://doi.org/10.1109/sbrn.2002.1181426
6. Meng Y, Yu X, He H, Tang Z, Wang X, Chen J. Knowledge-based modeling for predicting cane sugar crystallization state. International Journal on Smart Sensing and Intelligent Systems 7:942-965 (2014). https://doi.org/10.21307/ijssis-2017-689
7. Bakir T, Othman S, Puel F, Hammouri H. Continuous-discrete observer for crystal size distribution of batch crystallization process. Proceedings of the 44th IEEE Conference on Decision and Control :6240-6244 (None). https://doi.org/10.1109/cdc.2005.1583161
8. Georgieva P, Meireles MJ, Feyo de Azevedo S. Knowledge-based hybrid modelling of a batch crystallisation when accounting for nucleation, growth and agglomeration phenomena. Chemical Engineering Science 58:3699-3713 (2003). https://doi.org/10.1016/s0009-2509(03)00260-4
9. Meng Y, Yu S, Zhang J, Qin J, Dong Z, Lu G, Pang H. Hybrid modeling based on mechanistic and data-driven approaches for cane sugar crystallization. Journal of Food Engineering 257:44-55 (2019). https://doi.org/10.1016/j.jfoodeng.2019.03.026
10. Morales H, di Sciascio F, Aguirre-Zapata E, Amicarelli A. Crystallization process in the sugar industry: a discussion on fundamentals, industrial practices, modeling, estimation and control. Food Eng Rev 16:441-469 (2024). https://doi.org/10.1007/s12393-024-09377-3
11. Simoglou A, Georgieva P, Martin EB, Morris AJ, Feyo de Azevedo S. On-line monitoring of a sugar crystallization process. Computers & Chemical Engineering 29:1411-1422 (2005). https://doi.org/10.1016/j.compchemeng.2005.02.013
12. Morales H, Sciascio F, Aguirre-Zapata E, Amicarelli AN. A model-based supersaturation estimator (inferential or soft-sensor) for industrial sugar crystallization process. Journal of Process Control 129:103065 (2023). https://doi.org/10.1016/j.jprocont.2023.103065
13. Crestani CE, Bernardo A, Costa CBB, Giulietti M. Experimental data and estimation of sucrose solubility in impure solutions. Journal of Food Engineering 218:14-23 (2018). https://doi.org/10.1016/j.jfoodeng.2017.08.023
14. Hulburt HM, Katz S. Some problems in particle technology. Chemical Engineering Science 19:555-574 (1964). https://doi.org/10.1016/0009-2509(64)85047-8
15. Frew JA. Optimal control of batch raw sugar crystallization. Ind. Eng. Chem. Proc. Des. Dev. 12:460-467 (2002). https://doi.org/10.1021/i260048a013

16. Harrison RL, Granja C, Leroy C. Introduction to monte carlo simulation. AIP Conference Proceedings :17-21 (2010). https://doi.org/10.1063/1.3295638
17. “Development of the PID controller, ” *IEEE Control Syst.*, vol. 13, no. 6, pp. 58–62, Dec. 1993, doi: 10.1109/37.248006.
18. Borase RP, Maghade DK, Sondkar SY, Pawar SN. A review of PID control, tuning methods and applications. Int. J. Dynam. Control 9:818-827 (2020). https://doi.org/10.1007/s40435-020-00665-4
19. “An analysis package comparing PID anti-windup strategies, ” *IEEE Control Syst.*, vol. 15, no. 2, pp. 34–40, Apr. 1995, doi: 10.1109/37.375281.
20. Klyde D, McRuer D, Myers T. PIO analysis with actuator rate limiting. 21st Atmospheric Flight Mechanics Conference : (1996). https://doi.org/10.2514/6.1996-3432